14. Aging effects on source apportionment from the single particle perspective

i. Introduction

Landmark cohort studies published over a decade ago recognized an association between mortality and long term exposure to air pollution (specifically to particulate matter with diameters less than 2.5 μm or $PM_{2.5}$) (458,459), but improvements in recent epidemiological studies have allowed for better linkage between specific sources and their adverse health effects (460). Through understanding the health impacts and the ambient contributions to a particular region by specific sources (a process which is called source apportionment), government agencies can establish necessary regulations to effectively reduce the pollutants from targeted anthropogenic sources and, therefore, the negative health effects. The alternative for these agencies are blanket reductions, which are far more expensive and less effective than source-specific ones.

The majority of source apportionment methods rely on data from bulk aerosol sampling techniques coupled with off-line chemical analysis; these traditional receptor-orientated techniques include chemical mass balance (CMB) modeling, which utilizes unique nonreactive or stable tracer species, and factor analysis modeling by principal component analysis (PCA) or positive matrix factorization (PMF) (461-463). Recently, a new approach to source apportionment has been developed that compares all of the chemical information of individual ambient particles to the mass spectral signatures in a library of known sources (41,344). Designed for the single particle technique aerosol time-of-flight mass spectrometry (1), this new method has the advantage of producing size-segregated and high temporal resolution results. One of the potential challenges of using the source signature library approach involves its ability to accurately apportion aerosols that have "aged" or undergone atmospheric processing since being freshly emitted. Aerosol aging by physical and chemical processes such as reactive uptake, mass transfer, and condensed-phase processes can change the chemical composition and properties of individual particles (464,465). In fact, recent laboratory and field studies have demonstrated that the aging of aerosols increases their cloud condensation nuclei (CCN) activity or ability to form cloud droplets, which is part of one of the largest uncertainties in the radiation balance of the earth (466-470). The issue for source apportionment with the source signature library is whether or not the aging of a particle alters its chemical signature enough from that of the original source fingerprint that the particle is mislabeled or unassigned.

It has been established that the source signature library approach works successfully (matching 97% of the particles) for relatively "fresh" environments, such as directly alongside a major freeway (41,344). The goal of this study is to apply the library matching technique in order to evaluate and improve its performance on ambient measurements made during two different seasons (summer and fall) in the highly aged environment of Riverside, California. Located east and downwind of the Los Angeles (LA) Basin, Riverside is a receptor site for the LA air pollutants which have time to age during transport, as already described in Chapters 3 and 4. The source apportionment of Riverside represents an extreme challenge, as this environment is both highly polluted and aged. Two different approaches (lowering the "matching" factor and introducing

new aged source signatures to the library) to handling the aging effects of particles are examined. An area of particular interest in this study includes the aging effects on similar particle types, such as the combustion exhaust emissions of heavy duty diesel vehicles (HDDV) and light duty gasoline vehicles (LDV) which can be distinguished and separated under fresh conditions (38,41,344). Also in this study, which secondary chemical species on particles apportioned to such primary sources are dominate will be investigated.

ii. Experimental

a. Sampling location and instrumentation

Ambient sampling on the campus of the University of California, Riverside (33°58′18″N, 117°19′22″W) during the summer (July-August) and fall (October-November) of 2005 occurred in conjunction with the Study of Organic Aerosols at Riverside (SOAR) field campaign. Details on the sampling location and inlets of the mobile laboratory can be found elsewhere (31) and in previous chapters (3 and 4). Single particle size and chemical composition were measured by two collocated aerosol time-of-flight mass spectrometers (ATOFMS). An ultrafine ATOFMS (UF-ATOFMS), equipped with an aerodynamic lens system, detected particles with aerodynamic diameters between 50 and 400 nm, while a standard nozzle inlet ATOFMS measured particles with aerodynamic diameters between 140 and 3000 nm. Details of the transportable instrumentation have been described previously (1,2). During the summer, the UF-ATOFMS operated continuously from July 23rd to August 15th, whereas the standard ATOFMS ran from July 29th to August 15th. Both instruments operated from October 31st to November 21st during the fall season. All results are presented in Pacific Standard Time (PST), which is one hour behind local time during the summer.

b. Data analysis

During the SOAR campaigns, the combined ATOFMS instruments acquired millions of individual particle mass spectra. Using a matching function of the ART-2a clustering algorithm (35), these spectra were apportioned and classified based on their similarity to a set of predefined seeds (or signatures) based on the dot product of their vectors. ART-2a has a user-defined threshold parameter called the vigilance factor (VF), which represents the minimum degree of similarity necessary for a particle spectrum to match a seed; with a range of 0 to 1.0, the main VF used in this study (0.85) represents a relatively high VF value. The ambient particles are matched to predefined seeds in a source signature library, as developed and described in detail by Toner et al. (41,344). Briefly, this size-segregated source signature library contains mass spectral signatures from a series of source and ambient characterization studies (including vehicle dynamometer studies) for sources including HDDV and LDV exhaust emissions, dust, sea salt, biomass, and meat cooking. The representative seeds were made from the top (most populated) ART-2a clusters that accounted for ~90% of the particles in the datasets of the source characterization studies. For example, roughly 30 ART-2a clusters account for 90% of the particles in the HDDV (36-38,471) and LDV (36-38,471) studies. The library also contains non-source specific signatures such as aged elemental carbon (EC), aged organic carbon (OC), amine-containing particles, ammonium-rich particles,

vanadium-rich particles, EC, and polycyclic aromatic hydrocarbon (PAH)-containing particles. Certain specific sources, such as sea salt, dust, biomass burning, and meat cooking, have proven to be readily distinguishable in previous ATOFMS ambient characterization measurements; therefore, representative seeds for these particle types were made from several lab and ambient studies and incorporated into the library. The studies used to obtain the source signatures included: freeway 2004 (FWY) study (41,344), SOAR 1 & 2 (31), the Cloud Indirect Effects Experiment in Trinidad Head, CA (CIFEX) study (472,473), the ABC Post Monsoonal Experiment in Hanimaadhoo, Republic of Maldives (APMEX) study (474), and the Megacity Initiative: Local and Global Research Observations in Mexico City, Mexico (MILAGRO) study (475). The library is separated into three different size ranges, because there are distinct chemical differences for each source based on size. It was determined that these size ranges (50-100 nm, 100-140 nm, and 140+ nm) reflect the largest chemical, and hence source specific, differences. Currently, there are 322, 369, and 423 total seeds in the 50-100 nm, 100-140 nm, and 140+ nm libraries, respectively. **Table 17** provides the number of seeds used for each source in the original source signature library based on size.

After matching the ambient particles to the source signature library, a significant fraction of particles were not assigned to any category. Some of these unclassified particles had noisy spectra due to poor signal-to-noise ratios or erroneous peaks and need to be removed from the dataset. With cluster analysis, these particles form many clusters occupied by a single particle, because the peaks are noise and randomly occur at various mass/charge values. In order to isolate these noisy spectra in each size range, ~20,000 (due to computer memory limitations) unclassified particles spread temporally across the study were analyzed by ART-2a with a VF of 0.85. Of the resulting clusters, all singly-occupied clusters were removed, so that the remaining clusters could be used as seeds. Next, all of the unclassified particles in that size range were compared to these seeds at a VF of 0.85. All particles that did not match one of these seeds were removed from the dataset. This removal process was verified by selecting a different set of ~20,000 particles to create the seeds. The resulting unmatched particles agreed with the unmatched particles obtained from the first set of ~20,000 particles, indicating that the first set was indeed representative of all the unclassified particles in that size range. In the end, approximately 8.2% of the ~2.1 million particles obtained by the standard inlet ATOFMS and approximately 9.6% of the ~5.3 million particles obtained by the UF-ATOFMS were removed from all future analysis.

iii. Results and Discussion

a. Source signature library matching

The hourly temporal results from matching the ambient particles detected during

Table 17: Number of library seeds for each source per size range

Category	Source Study	UF (50-100 nm)		SAM (100-140 nm)		LAM, SUB, & SUPER (140-3000 nm)	
		# of Seeds	Seed Order in Library	# of Seeds	Seed Order in Library	# of Seeds	Seed Order in Library
HDDV	HDDV 2001 and 2003 dynamometer, FWY 2004	36	1-30, 35, 41-42, 45, 47, 58	71	1-60, 68, 337-339, 344-350	83	1-60, 68, 369-373, 375-378, 384-386, 391-394, 397-399, 402-404
LDV	LDV 2002 dynamometer, FWY 2004	24	31-34, 36-40, 43-44, 46, 48-57, 59-60	29	61-67, 69-90	29	61-65, 67, 69-81, 83-90, 395-396
Dust	APMEX, CIFEX, FWY 2004, SOAR2, Lab samples	129	84, 89-192, 197-209, 214-217, 287-293	129	114, 119-222, 227-239, 244-247, 317-323	129	114, 119-222, 227-239, 244-247, 317-323
Sea Salt	CIFEX, APMEX, FWY 2004, SOAR2	44	62, 67-69, 78-83, 85-88, 195-196, 210-213, 263-286	48	92, 97-99, 108-113, 115-118, 225-226, 240-243, 293-316, 340-343	48	92, 97-99, 108-113, 115-118, 225-226, 240-243, 293-316, 387-390
Biomass	CIFEX, FWY 2004, SOAR1	20	61, 63-66, 70-77, 193-194, 234-238	20	91, 93-96, 100-107, 223-224, 264-268	20	91, 93-96, 100-107, 223-224, 264-268
Aged EC	FWY 2004, SOAR1	2	227-228	2	257-258	3	257-258, 406
Aged OC	FWY 2004, SOAR1	5	229-233	8	259-263, 351-353	8	259-263, 383, 400-401
Amine	FWY 2004, SOAR1	17	218-221, 294-306	17	248-251, 324-336	18	248-251, 324-336, 407
NH_4 rich	SOAR1	2	222-223	2	252-253	2	252-253
Vanadium rich	FWY 2004, SOAR1, SOAR2	27	224-226, 239-262	27	254-256, 269-292	57	254-256, 269-292, 337-364, 379-380
EC (pos only)	FWY 2004	0		0		10	66, 82, 365-368, 374, 381-382, 405
Meat Cooking	FWY 2004, MILAGRO 2006	16	1-16* (separate order)	16	1-16* (separate order)	16	1-16* (separate order)

the summer and fall SOAR field campaigns to the original source signature library are shown in **Figure 104** and **Figure 105**, respectively. The results are size-segregated to better illustrate the size dependence of the different particle types. Size-segregated source apportionment also is useful for linking sources with specific health effects. The top three plots represent the relative chemical class fractions for ultrafine (UF: 50-100 nm), small accumulation mode (SAM: 100-140 nm), and large accumulation mode (LAM: 140-400 nm) particles as detected by the UF-ATOFMS. The last two plots provide the combined relative fractions for submicron (SUB: 140-1000 nm) and supermicron (SUPER: 1000-3000 nm) particles as detected by the standard ATOFMS. The missing periods (white effective density measurements (48), or low particle statistics in that hour (<10 particles). As additional information, **Figure 106** and **Figure 107** illustrate the matching process with the summer and fall data, respectively, by providing the number of particles that matched to each source seed in the library.

Of all the different size ranges, the plot for the ultrafine particles show the smallest percentage (~3%) of particles that did not match the source signature library at a VF of 0.85 or above, which are labeled as the unclassified particles. Actually, the initial percentage of unclassified ultrafine particles was ~64% mainly due to detector "crosstalk" issues. Detector "crosstalk" is produced in the UF-ATOFMS negative ion mass spectra due to the interference of extremely intense peaks in the positive polarity. These crosstalk issues are not accounted for in the source signature library; therefore, after the initial matching, the ~64% of unclassified particles were matched again to the bars) are due to instrument downtime for quality control procedures and maintenance, source signature library at a VF of 0.85 using only the positive mass spectral information

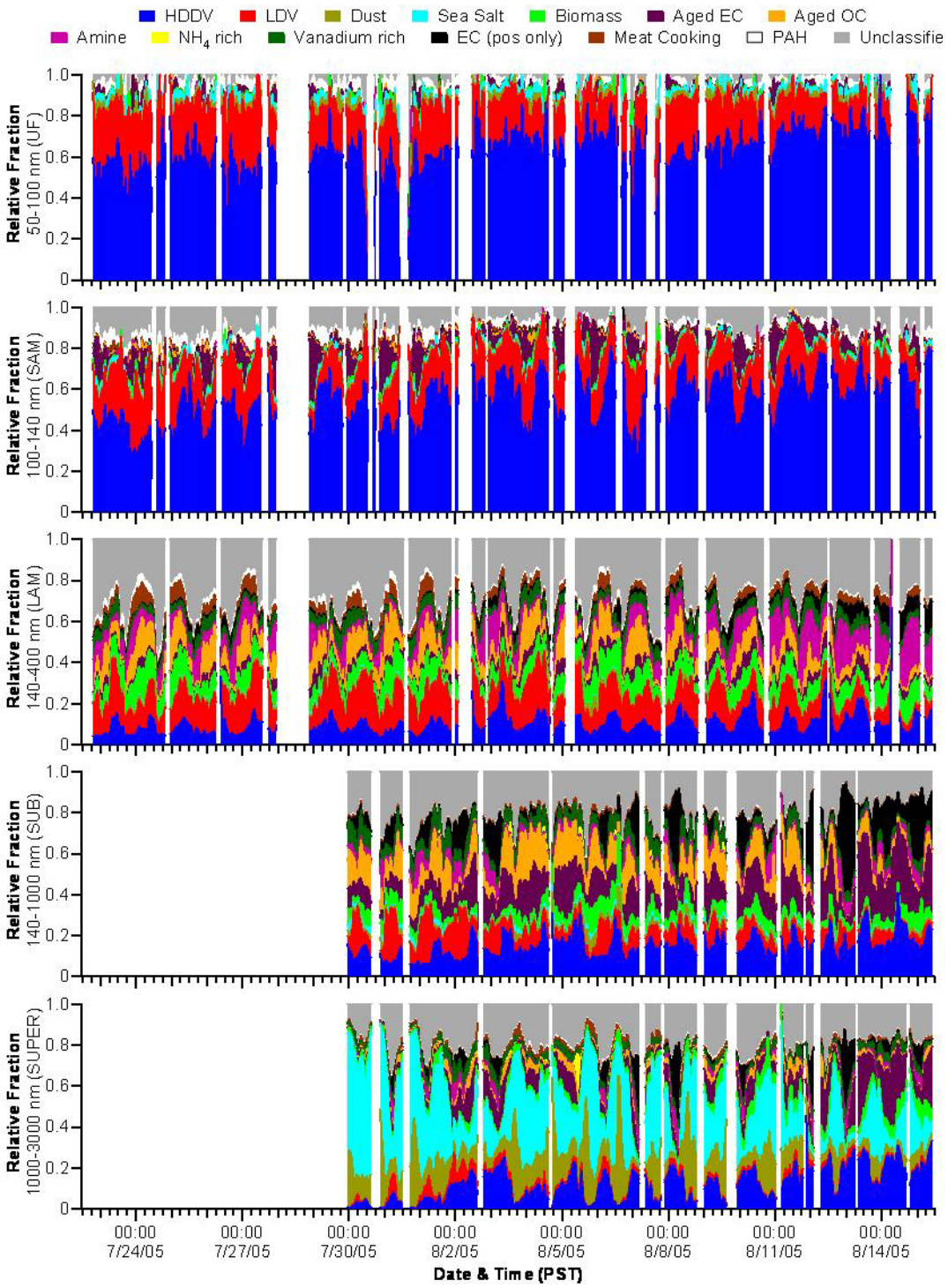

Figure 104: Hourly temporal series of the size segregated source apportionment fractions (VF = 0.85) for the summer SOAR ultrafine (UF), small accumulative mode (SAM), large accumulation mode (LAM), submicron (SUB), and supermicron (SUPER) particles detected with the UF-ATOFMS and ATOFMS.

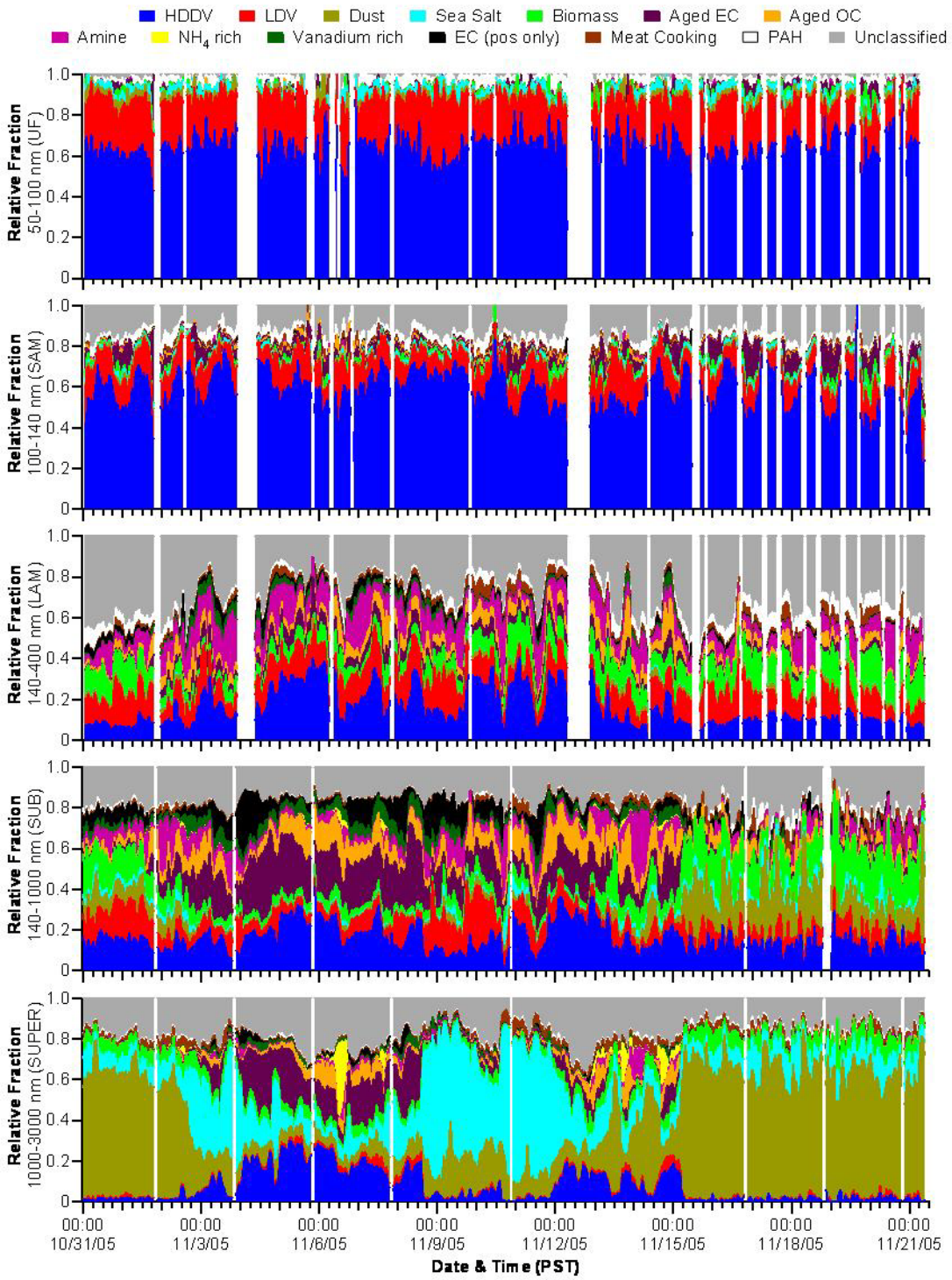

Figure 105: Hourly temporal series of the size segregated source apportionment fractions (VF = 0.85) for the fall SOAR ultrafine (UF), small accumulative mode (SAM), large accumulation mode (LAM), submicron (SUB), and supermicron (SUPER) particles detected with the UF-ATOFMS and ATOFMS.

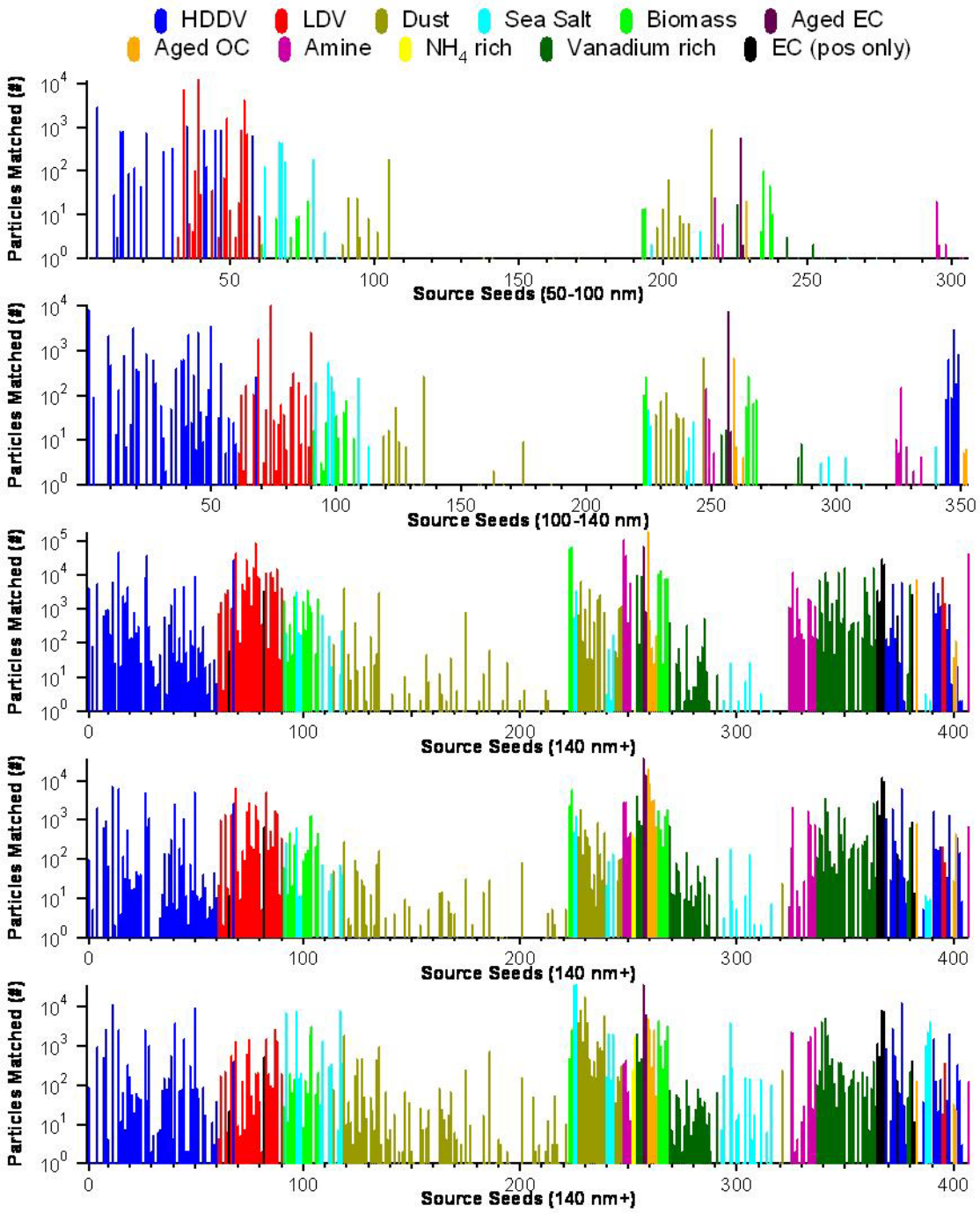

Figure 106: Number of summer particles matched to each source seed for a) UF (50-100 nm), b) SAM (100-140 nm), c) LAM (140-400 nm), d) SUB (140-1000 nm), and e) SUPER (1000-3000 nm) particles.

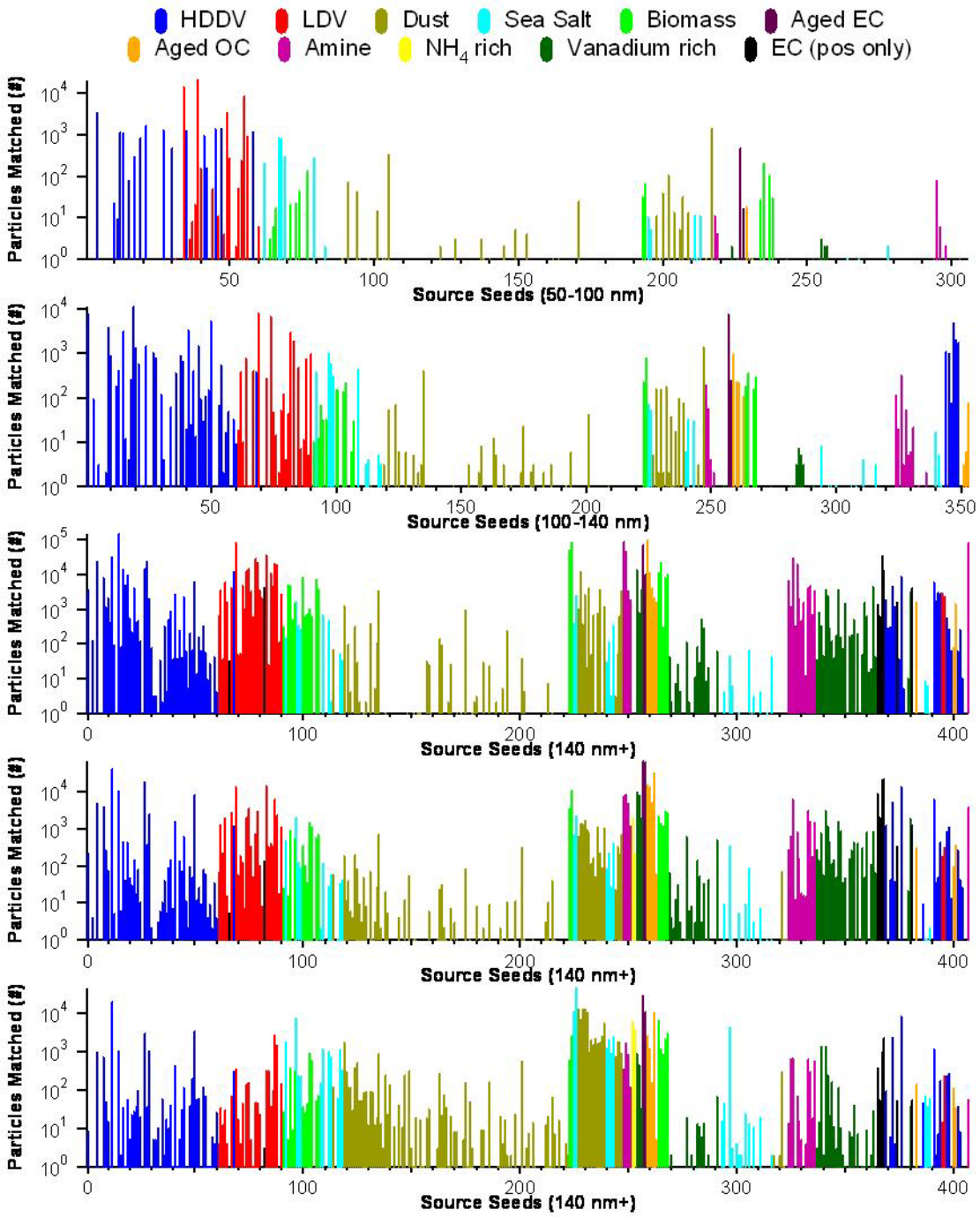

Figure 107: Number of fall particles matched to each source seed for a) UF (50-100 nm), b) SAM (100-140 nm), c) LAM (140-400 nm), d) SUB (140-1000 nm), and e) SUPER (1000-3000 nm) particles.

(344,476). As the ultrafine particles are the ones most strongly impacted by crosstalk issues, the second matching iteration using only positive ion information was performed only on this size range. The resulting relative fractions show that over 80% of the ultrafine particles are apportioned to vehicle exhaust emissions with the HDDV emissions being nearly three times that of the LDV emissions. Previous studies have

already shown that fresh local vehicle exhaust emissions are the dominant source of primary ultrafine particles in Riverside, though they did not distinguish between HDDV and LDV emissions (44,45). The ultrafine plots in **Figure 104** and **Figure 105** show that the relative contributions by HDDV and LDV exhaust emissions stay fairly constant with time. A focused study (Chapter 3) on the ultrafine particles observed during the SOAR campaigns determined that the raw number counts, rather than the relative percentages, of ultrafine particles detected by the UF-ATOFMS represent a good proxy for traffic activity (477). Although some of the particles in the 100 to 140 nm size range are also impacted by crosstalk issues, a second matching iteration with positive only information was not run on this size range. The spectra of ultrafine particles (seeds and ambient) are relatively simple and chemically pure, which allows the positive only matching to work well. When the spectra become more complex (as with particles of a larger size), the results from positive only matching become less reliable. When manually inspecting the unclassified category left after matching the 100 to 140 nm particles to the source signature library, it was determined that the top unclassified type was impacted by crosstalk issues and that this type belonged in the HDDV category. The positive ion spectra of this top type contained an elemental carbon with calcium signature that closely resembled one of the dominant chemical classes from HDDV exhaust emissions during dynamometer studies (36-38,471). Therefore, the SAM results shown in **Figure 104** and **Figure 105** include the matching results from the source signature library and the top crosstalk particle type that was manually added to the HDDV category.

As particle size increases, the relative fraction of particle apportioned to HDDV and LDV become less dominant and the contributions of the other particle types emerge. For example, **Figure 104** and **Figure 105** illustrate that for the two size ranges covering 140-1000 nm, there is no obvious prevailing particle source, as none of them (excluding the unclassified category) contribute more than 16% of the ambient particles, indicating that submicron ambient Riverside particles originate from a mixture of sources. On the other hand, the supermicron size ranges for both summer and fall are clearly dominated by the mechanically-generated sources of sea salt (26.3% and 19.8%) and dust (13.0% and 33.0%). As described in Chapter 1, it is expected that the mechanically-generated sources, such as sea salt and dust, dominate the supermicron size range, whereas particles from combustion and chemical processes dominate the submicron size range. It is worth noting that the percentage of Riverside particles apportioned to the aged non-source specific particle types (aged EC, aged OC, amine, and NH_4 rich: ~27% of the 140-1000 nm size range) is far greater than at sampling sites in Athens, Greece (August 2003) and Mexico City, Mexico (March 2006), due to the aged nature of the particles that have advected across the LA Basin (476). This observation shows how highly aged the ambient environment is in Riverside, compared to these other large urban cities. A more detailed view of how highly aged the Riverside aerosol is will be examined in the next section.

As mentioned earlier, Riverside is typically downwind of the LA Basin due to an onshore flow. However, seasonal differences are expected based on two distinct meteorological conditions involving a high pressure system over the desert areas that occur primarily in the fall and winter months: a weak system counterbalances the onshore flow, creating stagnant conditions; and under a strong system, there are warm and dry easterly (offshore) winds, known as Santa Ana winds (204). Both of these conditions

were observed during the fall SOAR field campaign. In fact, the summer measurements followed a diurnal pattern, whereas the measurements made during the fall season were episodic (31). These seasonal differences are clearly illustrated in **Figure 104** and **Figure 105**, especially with the larger sized particles. During the Santa Ana wind periods at the beginning (October 31 0:00 – November 1 19:00) and end (November 15 5:00 – November 21 10:00) of the fall study, resuspended dust was the dominant supermicron source as the easterly winds crossed the deserts before reaching Riverside. Qin et al. reported stagnant conditions from November 1 19:00 – November 7 18:00 during a buildup and high mass periods, when the hourly $PM_{2.5}$ mass concentrations reached 106 $\mu g\ m^{-3}$ which clearly exceeded the 24-hour national ambient air quality standard of 35 $\mu g\ m^{-3}$ (31). During this time frame, the aged EC particle type made its strongest contribution to both the submicron and supermicron size ranges. Additionally, there was an extremely strong spike in NH_4 rich particles; the nearby Chino dairy area is the largest single source of ammonia emissions in the LA area (150). The particles during this spike have intense ammonium and nitrate cluster peaks. The smallest size ranges shown in **Figure 105** show little episodic variation. These fresh emissions are mainly dependent on very local sources, and, as described in Chapter 3, their *number* concentrations do vary but this trend is not reflected in the relative percentage plots.

b. Aging effects

Particles in the unclassified category were examined closely to determine why these particles were not apportioned to either a primary source or a non-source specific class using the original source signature library. There are a few reasons why a particle may have not been classified: crosstalk issues (as discussed above), miscalibrations in the spectra, or no appropriate seed exists in the source library. Miscalibrations occur when the peak area is listed under the incorrect *m/z*; often the mass spectral information is shifted by a single unit as in the common example of observing the $^{62}NO_3^-$ peak at *m/z* -61. Even though the peaks may be shifted by only one unit, the dot product of a miscalibrated spectrum with a source seed will yield a very different (lower) value than that of a properly calibrated spectrum. How often miscalibrations affect the spectral information varies from dataset to dataset. The lack of the proper seeds in the source library could be due either by missing sources that have yet to be characterized and added to the library or by heavy aging of the particles. The source library does contain some pseudo-aged signatures of the primary sources (41,344). These aged signatures did a fair job of matching the aged particles from primary sources, because the majority of the properly calibrated unclassified particles are heavily aged and would best fit in the aged non-source specific categories (mainly aged OC and amine). Because the purpose of this study is to understand how aging impacts the source apportionment results, aged particles that ended up in the unclassified category are the primary focus.

One approach to decreasing the percentage of aged particles that are placed into the unclassified category is to the lower the matching factor used with the source library. To examine how lowering the matching factor impacts the apportionment results, **Figure 108** provides the average source contribution pie charts when the ambient particles are matched with a VF of 0.85 or a VF of 0.75. Lowering the matching factor does reduce the percentage of unclassified particles, but previous error analysis has shown that the percent of error in properly apportioning 100 nm+ particles increases nearly fourfold

when using a VF of 0.75 instead of 0.85 (41,344). The percent error continues to increase with lower and lower VF values. An example of how the lower matching factor increases the error in apportionment is illustrated in **Figure 109**. This figure shows the average mass spectral information of summer particles in the 140 to 400 nm size range that were apportioned to the LDV category. The top plot (red) shows an average mass spectrum for all particles in that size range that were apportioned to LDV at a matching factor of 0.85. The middle plot (blue) shows an average mass spectrum for all of the additional particles that matched to LDV when the matching factor was lowered to 0.80 from 0.85. Likewise, the bottom plot (green) shows an average mass spectrum for all of the additional particles that matched to LDV when the matching factor was lowered to 0.75 from 0.80. **Figure 109** illustrates that the particles that were added to the LDV category when using a lower matching factor than 0.85 have mass spectral signatures that are more indicative of an aged OC particle type than that of LDV exhaust emissions. It is

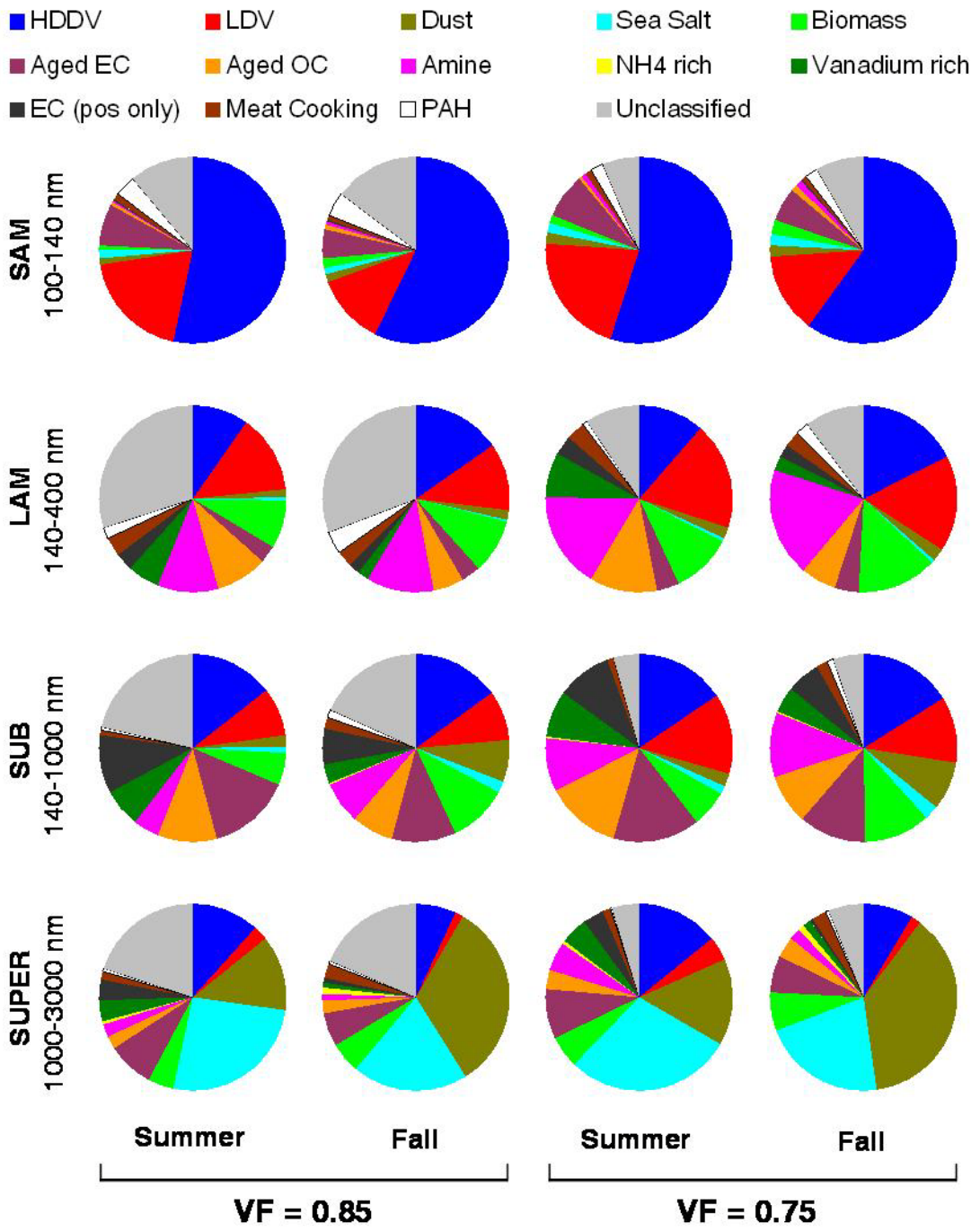

Figure 108: Average source contribution particles matched to the source library at different VF per size bin.

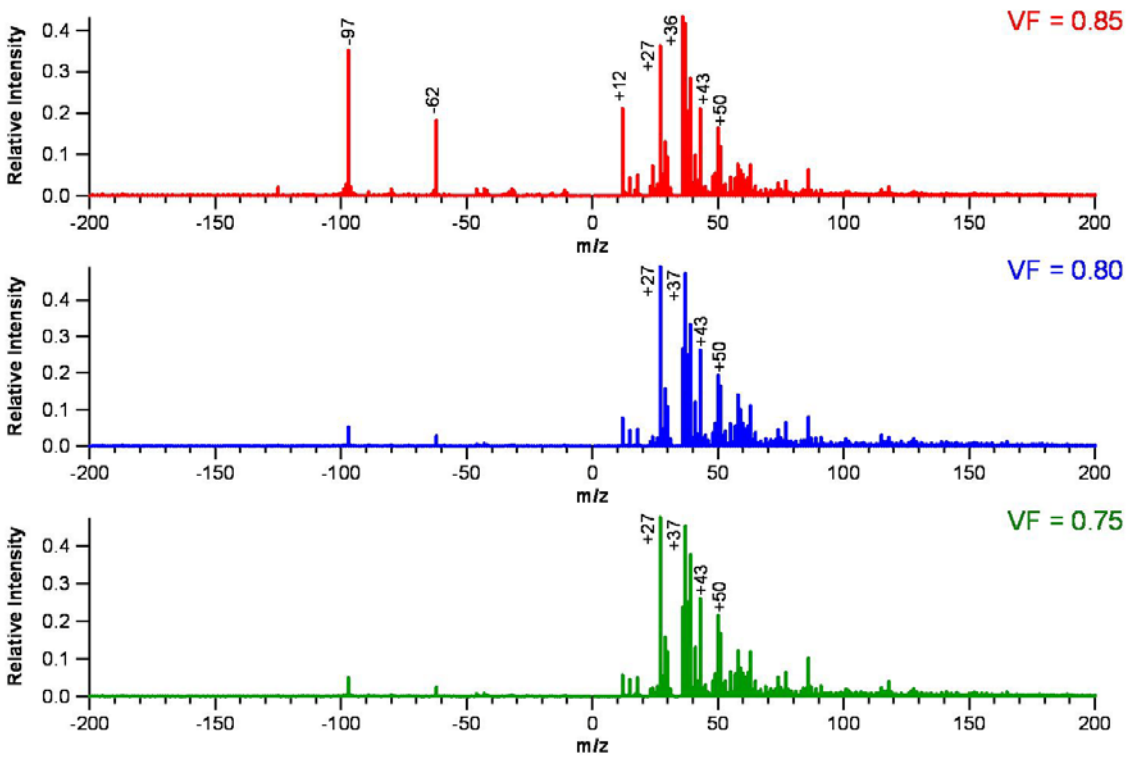

Figure 109: Average mass spectra obtained by lowering the matching factor for summer SOAR LAM (140-400 nm) particles apportioned to LDV.

possible that some of these additional particles are indeed aged LDV particles, but until controlled laboratory experiments can verify that this is the signature of aged LDV particles, they are being falsely labeled as LDV and should be in the aged OC category. Additional figures like **Figure 109** for LDV and HDDV particles in the other size ranges are provided in the Appendix.

The better method to reduce the unclassified category is to add appropriate seeds to the library and to use a matching factor of 0.85. By adding more aged seeds to the source library, the apportionment results of ambient particles in aged environments will have smaller fractions of unclassified particles and better estimations of the aged categories. The new aged seeds were created from the ART-2a results (VF = 0.85) of the unclassified category. ART-2a was run separately on the SAM, LAM, SUB, and SUPER unclassified particles for both summer and fall datasets. The top 30 clusters resulting from each of these ART-2a runs were manually examined to find all aged particle types that were not miscalibrated. A total of 47 properly calibrated aged seeds (22 for aged OC, 16 for amine, 7 for aged EC, and 2 for NH_4 rich) were found and all were added to both the 100-140 nm and 140+ nm size ranges of the source library. These seeds were not added to the ultrafine size range of the library, because particles of this small size are still relatively fresh and show little sign of aging. In fact, when the aged seeds were added to the ultrafine source library for testing purposes, it was determined that these additional seeds impacted the apportionment of less than 0.2% of all the ultrafine particles, thus justifying that the aged seeds need not to be added to the ultrafine size

range of the library. All particles (except for ultrafine particles) were matched to the updated source library, and the temporal results are shown in **Figure 110** and **Figure 111**.

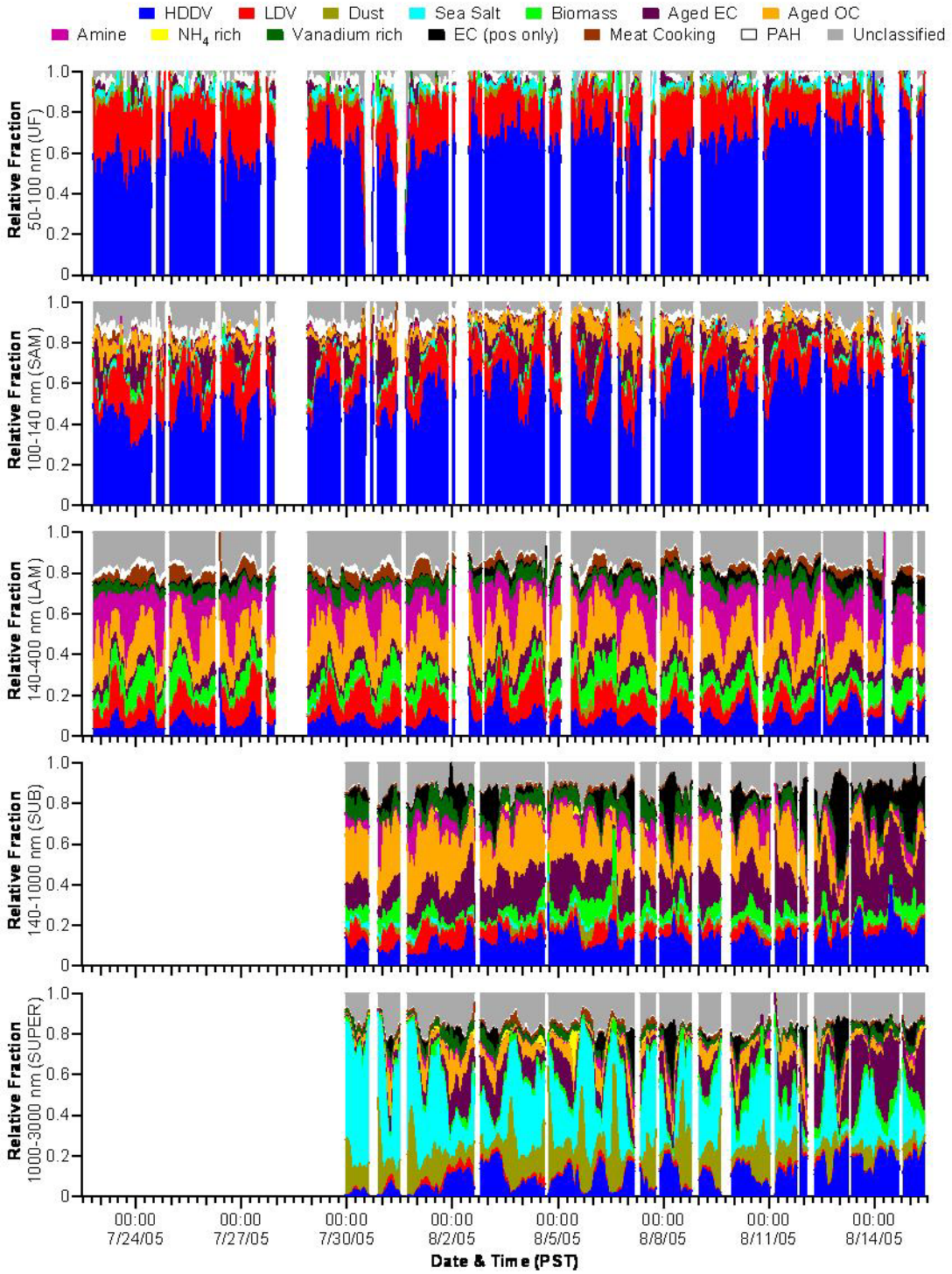

Figure 110: Hourly temporal series of the size segregated source apportionment fractions (VF = 0.85) for the summer SOAR ultrafine (UF), small accumulative mode (SAM), large accumulation mode (LAM), submicron (SUB), and supermicron (SUPER) particles using the updated source signature library.

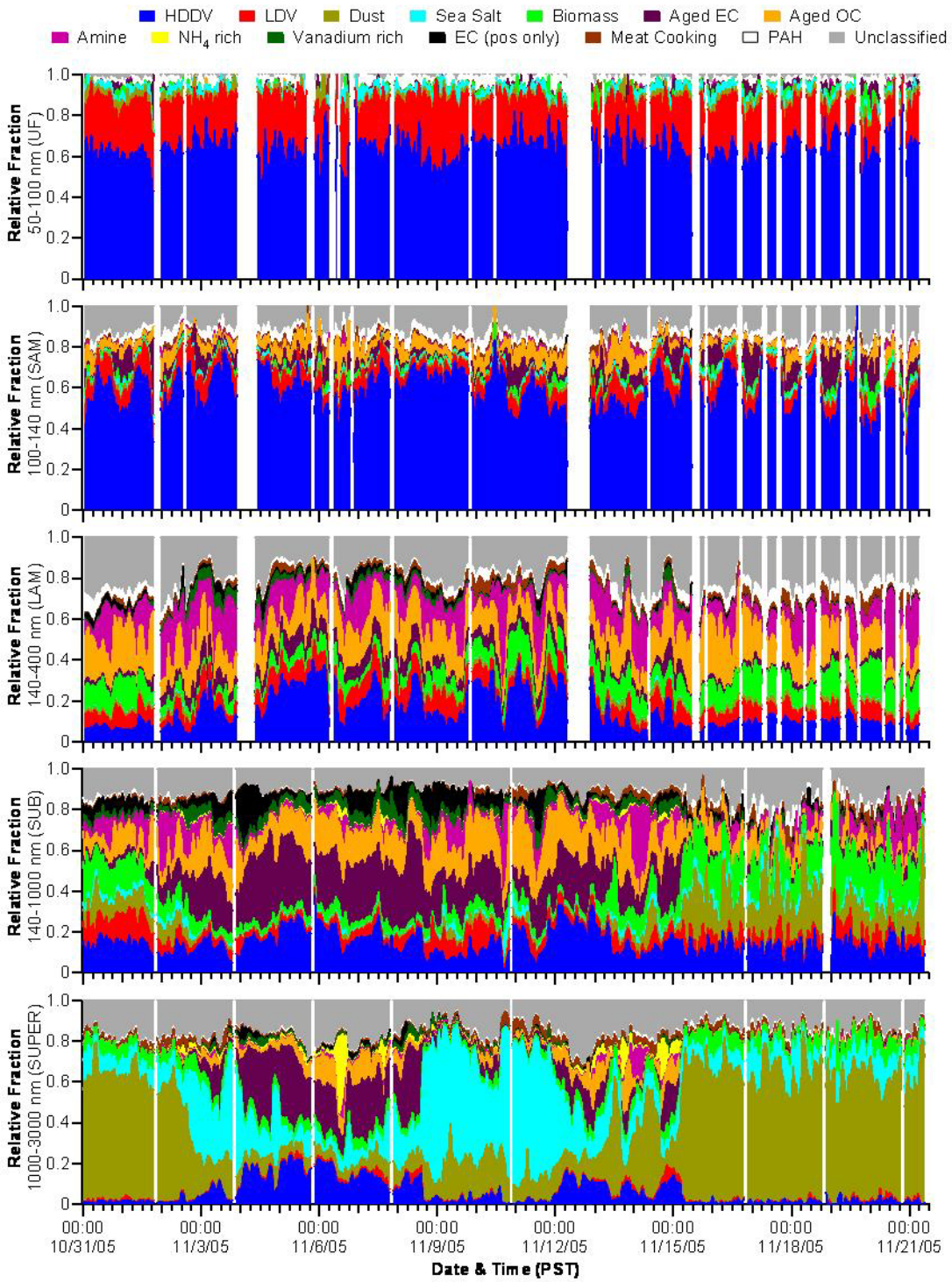

Figure 111: Hourly temporal series of the size segregated source apportionment fractions (VF = 0.85) for the fall SOAR ultrafine (UF), small accumulative mode (SAM), large accumulation mode (LAM), submicron (SUB), and supermicron (SUPER) particles using the updated source signature library.

	SAM (100-140 nm)		LAM (140-400 nm)		SUB (140-1000 nm)		SUPER (1000-3000 nm)	
	Summer	Fall	Summer	Fall	Summer	Fall	Summer	Fall
HDDV	-0.2	-0.2	-1.4	-1.0	-1.4	-1.2	-1.8	-1.4
LDV	-4.3	-5.2	-4.4	-4.9	-3.2	-2.9	-0.9	-0.3
Dust			-0.1					
Sea Salt					-0.1			
Biomass			-0.2	-0.1		-0.1		
Aged EC	+0.6	+0.7	+2.6	+1.6	+3.5	+3.4	+3.3	+2.3
Aged OC	+5.5	+5.7	+9.6	+10.8	+8.4	+6.0	+4.0	+1.3
Amine	+0.2	+0.2	+7.9	+3.1	+1.8	+0.6	-0.6	-0.2
NH_4 rich					+0.1	+0.2	+0.2	+0.4
Vanadium rich			-0.1		-0.1			-0.1
EC (pos only)	-0.2	-0.1	-0.3	-0.2	-0.7	-0.7	-0.3	-0.1
Meat Cooking								
PAH	-0.1	-0.1	-0.1	-0.1	-0.1			
Unclassified	-1.5	-1.2	-13.7	-9.4	-8.2	-5.2	-3.9	-1.9

Table 18: Percent difference between particles matched to the original source library and particles matches to the updated source library.

Table 18 provides the percent differences of matched particles to each category between using the old and the updated source libraries. Negative values indicate how much the percent of particles matched to that category dropped with using the updated library, whereas positive values indicate how much the percent of particles matched increased. The figures and table illustrate that not only were the percentage of particles matched to the aged categories increased and the percentage of unclassified particles decreased, but they also show that the percentage of particles apportioned to other categories (mainly LDV and HDDV) was also impacted by the addition of the aged seeds to the library. This result was expected, because the LDV seeds are largely OC and the HDDV seeds are largely EC. Some of aged ambient particle (aged OC and aged EC) could have matched these "fresh" OC and EC signatures, because they did not have a better alternative. However, with the addition of the new aged seeds, they matched the new signatures better (with a higher dot product value) and were properly placed into the aged categories. For example, it would be expected that the fraction of fresh OC (LDV) particles in the accumulation mode would be less at this location than another sampling site located closer to the major freeway; in fact, the average LAM LDV percentage at a roadside study during the summer (18.4%) is double the equivalent percentage (9.2%) in Riverside during the summer (41,344). The shift of LDV particles to the aged OC category was most highly anticipated for particles in the supermicron size mode, because on-road and laboratory (dynamometer) studies of LDV exhaust indicate that the number of particles emitted by gasoline or spark ignition engine fall off significantly well before 1000 nm (478,479). Therefore, it was expected that the LDV contribution to supermicron particles would be very small, which is the case (~1%). Kittelson and coworkers show that the number of particles emitted by diesel engines does not drop off as rapidly as those from gasoline engines [*Kittelson et al.*, 2006], which explains why the HDDV contribution to supermicron particles is much larger than the LDV contribution.

The improved source library successfully reduced the large spikes of unclassified particles during the afternoon/evening periods that were especially predominant in **Figure 104** (summer season). **Figure 110** shows that the contribution of aged types

(mainly aged OC and amine) are strongest during this time of day, as expected in the summer. Now the source apportionment results more closely match the hand-classified ART-2a results presented in Qin et al. (31). For example, Qin and coworkers determined that the average contribution of the aged OC and amine classes in the submicron size range during the summer was 40-45% by manually classifying the top 50 populated clusters from running ART-2a analysis at a VF of 0.80, and the combined contribution as determined by the updated source library for submicron particles during the summer was ~37%. Similarly, the average contribution of the aged OC and amine classes in the submicron size range during the fall was ~25% by manual classification and ~21% by the source library. The ART-2a method is slightly higher, because some of the fresh OC particles were placed into the aged OC clusters at the lower VF value and also the miscalibrated spectra were added to the appropriate category. The source signature library contains no miscalibrated seeds, so these ambient particles are currently placed in (and make up the majority of) the unclassified category. Improvements are presently being made on the peak writing program to reduce the number of particles with miscalibrated spectra. The remaining properly calibrated particles in the unclassified category (~35%) from using the updated source library are unique types for which there is no appropriate seed, such as the unique OC type with Ba that was described in Chapter 9. As more sources are characterized in future studies, new seeds (and source categories) can be added to the library, which will further reduced the unclassified category.

This episodic behavior of the fall season can be further examined by comparing the source contributions based on the different air masses. Using HYSPLIT (HYbrid Single-Particle Lagrangian Integrated Trajectory) model analysis, it is possible to determine the back trajectories of air masses arriving at the sampling site at specified heights (305). The 48 hour back trajectories at a starting height of 100 m (also verified at 500 m) were calculated for each hour of the study so that the air masses could be separated into 6 regions of origin. Representative back trajectories for each region are shown in **Figure 112**. Most air masses during the summer had LA and marine influences, though some traveled north along the Baja, San Diego (SD), and LA coastline or through Baja (inland) and over the Salton Sea (SS). On the other hand, the air masses sampled during the fall derived from all directions around Riverside, including from the San Joaquin Valley (SJV) in central California. Starting in Canada, the long trajectory representing the Santa Ana air masses illustrates how quickly these air masses transported to Riverside. The short trajectory representing the Northeastern (NE) Desert air masses indicates how stagnant they were. Under these stagnant conditions, higher concentrations of NH_4 rich particles are expected, as shown in **Figure 113**. This figure provides the relative source fraction based on HYSPLIT region and size range. Also as expected, the dust and sea salt apportionments are at their highest and lowest under the

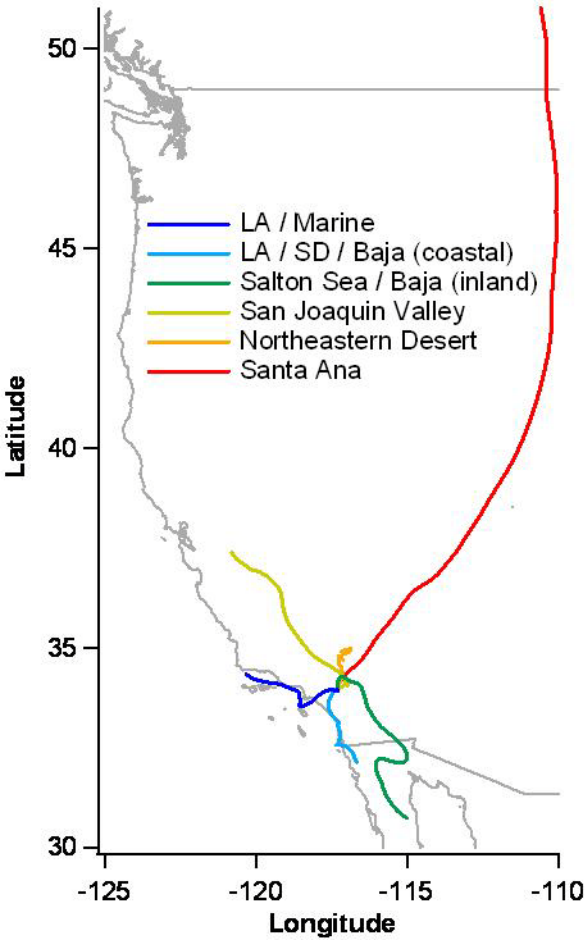

Figure 112: Representative 48 hour HYSPLIT back trajectories at a height of 100 m for six defined regions. (LA = Los Angeles, SD = San Diego)

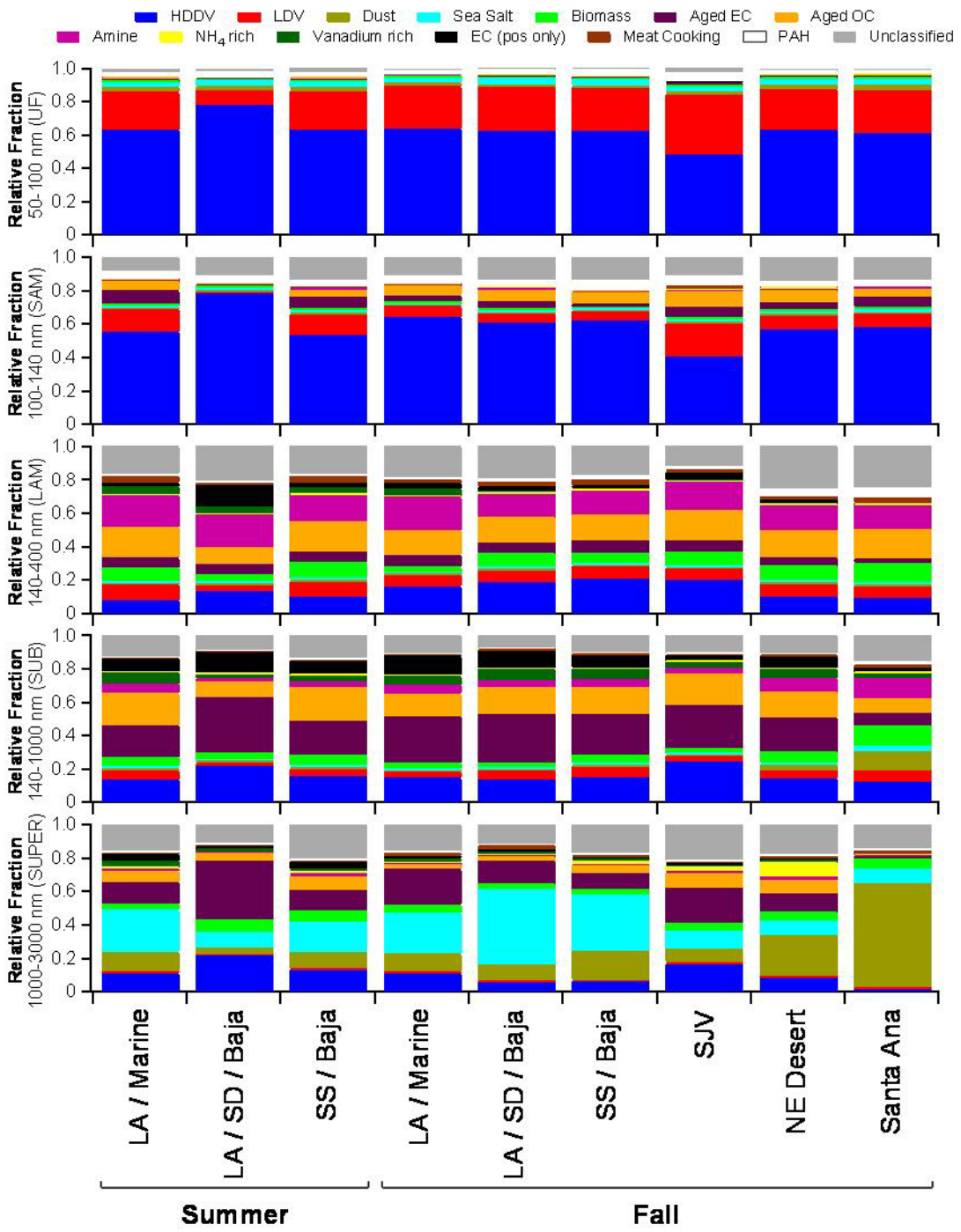

Figure 113: Relative class abundance based on air mass origin and size range. (LA = Los Angeles, SD = San Diego, SS = Salton Sea, SJV = San Joaquin Valley, NE = Northeastern)

c. Secondary species as aging markers

Since many of the Riverside aerosol particles are aged due to being freshly emitted in a highly aging environment, it is interesting to examine the extent of aging for particles apportioned to a source. There are a number of markers that can indicate the presence of specific secondary species. For example, the peak at *m/z* $^{18}NH_4^+$ indicates the presence of

ammonium, the peak at *m/z* $^{43}C_2H_3O^+$ indicates oxidized organic compounds, and the peak at *m/z* +86 commonly indicates the presence of amines in ATOFMS data. For the negative ion peaks, nitrate species are denoted by peaks at *m/z* $^{46}NO_2^-$, $^{62}NO_3^-$, or $^{125}H(NO_3)_2^-$ and sulfate by $^{97}HSO_4^-$. By comparing how the average amount of these secondary species adjusts with increasing size for each source, it should be possible to infer how the chemistry of particles of a particular source influences the aging processes. Based on the source characterization studies, it is already known that the original particle chemistry from HDDV (more EC) and LDV (more OC) is different, so the particles from these two types of vehicle exhaust can be expected to age differently (36-38,471). **Figure 114** shows the average area of these secondary markers (for both the UF-ATOFMS and ATOFMS data combined) on particles matched to the top primary sources (HDDV, LDV, dust, sea salt, and biomass) using the updated aged library. Particles detected by UF-ATOFMS cover the 50 to 400 nm range in 50 nm bins, and particles detected by the

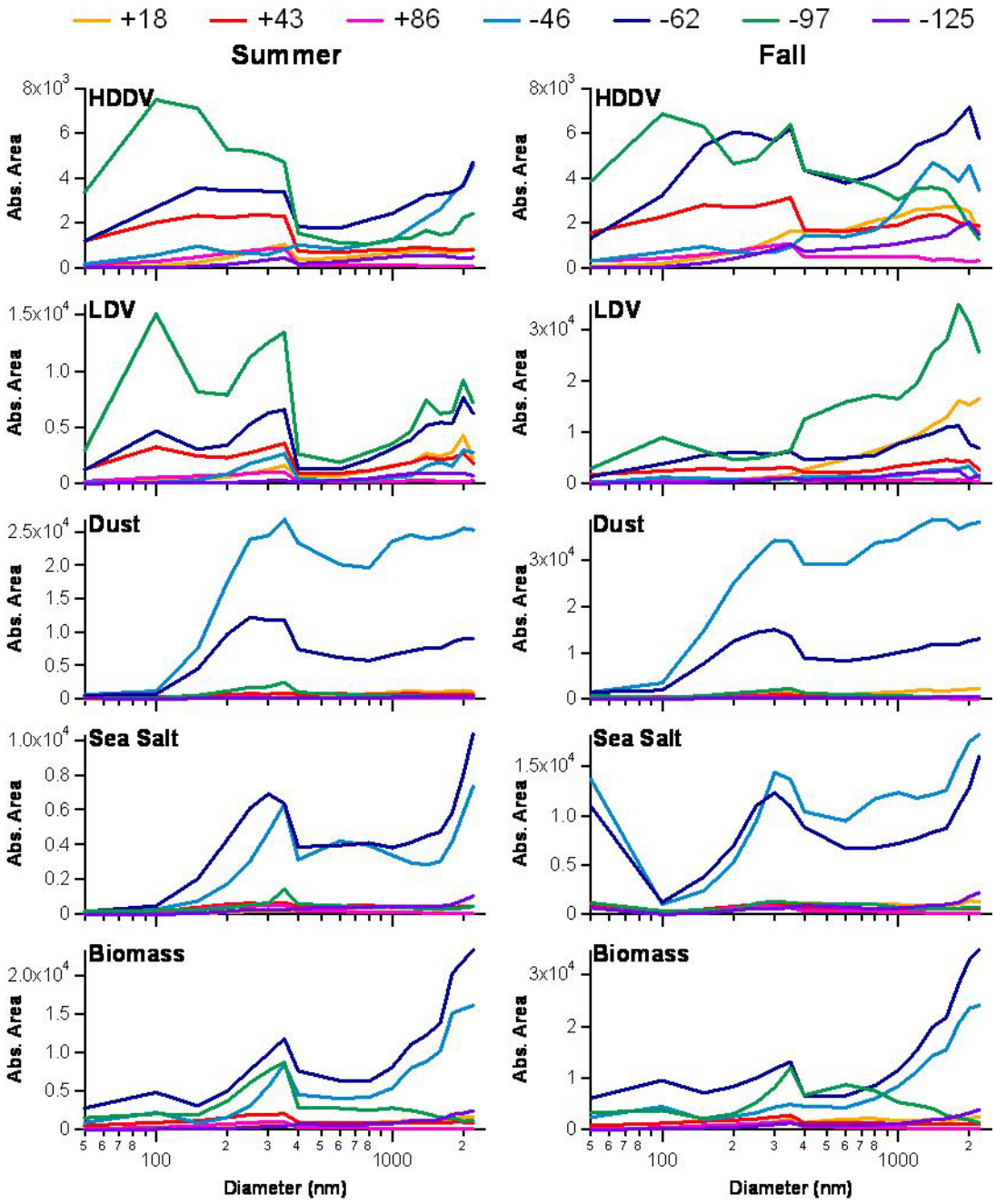

Figure 114: Size-resolved average area of secondary markers for particles matched to specific sources during the summer (left column) and fall (right column).

standard inlet ATOFMS cover the 400 to 2400 nm range in 200 nm bins. Some of the plots display a jump around 400 nm due to the transition between instruments measuring different size range. Each source has its own plot for both summer (left column) and fall (right column) measurements.

The average areas for several of the secondary species remain rather constant across all size bins above 100 nm. They include the relative areas for +43, +86, -125 and

sometimes +18. Therefore, there must be little addition of oxidized organics and amines as the particles emitted by these sources grow compared to nitrate and sulfate. Recall that particles whose spectra had significant amounts of +86 (heavily aged) were separately apportioned to the amine class. On the other hand, the average area markers for the secondary species of nitrate (-46 and -62) and sulfate (-97) do show changes with particle size and account for significant amounts of negative ion intensities. The general trend for all sources is an increase in the area of nitrate with increasing diameter. For most of the sources, the nitrate marker at *m/z* -62 is the dominant secondary species. This finding is not surprising, because in a previous study in nearby Mira Loma, it was determined that nitrate contributed to 26% of the total $PM_{2.5}$ mass (480). Large quantities of the reactive gas NO_2 are transported across the LA Basin. The plots in **Figure 114** suggest that there are different seasonal sources or mechanisms of nitrate on Riverside particles. During the fall season, the area of ammonium increases with the increasing diameter of HDDV and LDV particles, whereas the ammonium area stayed relatively flat for the same particles during the summer. This observation implies that while ammonium nitrate is important during the fall season, there is a different photochemical source of nitrate during the summer or that HNO_3 partitions with some other species during the summer, besides ammonium and amines (also flat). It is also interesting to note that -46 is the dominant nitrate peak on dust. In the ATOFMS reference mass spectra of unprocessed mineral dusts (obtained by analyzing Asian dust samples collected from various source regions), the peak at *m/z* -46 $[NO_2]^-$ is the only nitrate ion detected and there is no significant peak at *m/z* -62 (134). As with dust, nitrate represents the main secondary species on sea salt particles. Neither dust nor sea salt indicate a significant presence of sulfate. In previous ATOFMS studies of sea salt particles, sulfate has been observed at *m/z* 165 $[Na_3SO_4]^+$; however, this peak is not significant for other particle types and, thus, was not chosen as a marker of focus. The lack of sulfate (at *m/z* -97) on the dust particles contrasts the observation of large sulfate ion signals on ambient aged dust particles analyzed aboard a ship in the Pacific Ocean during the ACE-Asia campaign (134). One of the key findings of that study was that dust particles could contain large amounts of either nitrate or sulfate but rarely would they contain both ions (134,481). On the other hand, sulfate is shown on particles of HDDV and LDV emissions during the SOAR campaign, but not for dust and sea salt particles. Understanding which particle types are internally mixed with sulfate is important, because sulfate associated particles have been shown to have the potential to modify the radiation budget of the atmosphere (482). Relatively fresh emissions of HDDV, LDV, and biomass burning already show the presence of sulfate ions (36-38,471), so *m/z* -97 can also represent primary sulfate. However, sulfate on dust could be secondary in nature. In Riverside, there is no sulfate present on dust, because the LA Basin has less SO_2 than locations in and nearby Asia (due to coal-fired power plants). A modeling study determined that the available surface area is a critical factor in the preferential deposition of secondary sulfate by SO_2/H_2SO_4 (12). In locations such as Riverside, the particle types with the most available surface area dominate the submicron size mode, and so if there were any significant secondary sulfate, it would prefer the carbonaceous types (HDDV, LDV, and biomass). In fact, this preference may explain the seasonal differences with the sulfate marker for LDV particles. The peak in average area for sulfate occurs in smaller sized LDV particles during the summer than in the fall.

In summary, a source signature library was used to determine the relative contributions of primary sources and non-source specific types to ambient particles collected in Riverside during the summer and fall of 2005. It was determined that local vehicle exhaust emissions (specifically HDDV) account for the majority of the small (50-140 nm) particles detected. Varying meteorological conditions caused seasonal differences in the apportionment of the larger (140+ nm) particles during the summer (diurnal trends) and fall (episodic behavior). These results were supported by the air mass back trajectories calculated with HYSPLIT. The main impacts of aging effects on the original source apportionment results were an increase in the unclassified fraction and thereby an underestimation of the contributions by aged non-source specific types. Therefore, it was determined that the aging of a particle can alter its chemical signature enough so that the particle is unassigned. Adding aged seeds obtained from this dataset to the source signature library did reduce the impact of aging effects and improved the ability of the source signature library to perform successfully for future source apportionment studies in highly aged environments. Depending upon the size range, these additional seeds reduced the percentage of unclassified particles by ~1 to 14% and increased the percentage of particles categorized to aged categories by ~4 to 20%. Finally, a close examination of markers of secondary species revealed that nitrate, despite having different seasonal sources, is the dominant secondary species for aged particles from all of the primary sources in Riverside.

iv. Acknowledgements

The authors express their gratitude to the entire Prather group for their help in the preparation and overall support of these studies. We thank Megan McKay and the Goldstein research group at the University of California, Berkeley for the meteorology data. We also acknowledge Professor Paul Ziemann (University of California, Riverside) for hosting the SOAR field campaigns, as well as Professor Jose Jimenez (Colorado University, Boulder) and Dr. Ken Docherty (Colorado University, Boulder) for setting up the logistics. We express gratitude to the NOAA Air Resources Laboratory (ARL) for the provision of the HYSPLIT transport and dispersion model. Funding for this project was supplied by the California Air Resources Board (Contract 04-336).